Copolymerization of Cyclic Esters Controlled by Chiral NNO-Scorpionate Zinc Initiators.

Antonio Otero,[*,†] *Juan Fernández-Baeza,*[*,†] *Luis F. Sánchez-Barba,*[*,‡] *Manuel Honrado,*[†] *Andrés Garcés,*[‡] *Agustín Lara-Sánchez*[†] *and Ana M. Rodríguez*[†]

[†]Departamento de Química Inorgánica, Orgánica y Bioquímica, Universidad de Castilla-La Mancha, Campus Universitario, 13071-Ciudad Real, Spain.

[‡]Departamento de Biología y Geología, Física y Química Inorgánica, Universidad Rey Juan Carlos, Móstoles-28933-Madrid, Spain.

E-mail: antonio.otero@uclm.es; juan.fbaeza@uclm.es; luisfernando.sanchezbarba@urjc.es

RECEIVED DATE (to be automatically inserted after your manuscript is accepted if required according to the journal that you are submitting your paper to)

ABSTRACT

Reaction of chiral alcohol-scorpionate compoundbpzteH [bpzteH = 2,2-bis(3,5-dimethylpyrazol-1-yl)-1-*para*-tolylethanol] with [ZnR_2] (R = Me, CH_2SiMe_3) in a 1:2 molar ratio afforded the dinuclear chiral alkyl zinc complexes [Zn(R)(κ^2-NNμ-O)Zn$(R)_2$] (**1**–**2**) [κ^2-NNμ-O= bpzte, R = Me **1**, CH_2SiMe_3**2**]. Using these trialkyl complexes in an alcoholysis reaction with ArOH (1 equiv; Ar = 2,6-$C_6H_3Me_2$) yielded the chiral dinuclear zinc complexes [$(ZnR)_2$(κN:κN-μ-O)(μ-EAr)] (**3**–**4**) [κN:κN-μ-O= bpzte, R = Me **3**, CH_2SiMe_3**4**]. The structures of the different compounds were determined by spectroscopic methods and, in addition, the X-ray crystal structures of **1** and **3** confirmed a dinuclear structure in all complexes, with the alkoxide of the heteroscorpionate ligands in a μ-bridging mode between the two Zn(II) centers.

Trisalkyl and alkyl-aryloxide-containing zinc complexes **1**–**4** can act as single-component initiators for the ring-opening homopolymerization of ε-caprolactone and L-/*rac*-lactide, affording materials with low molecular weights and narrow monomodal molecular weight distributions under mild conditions in only a few hours. Microstructural analysis of poly(*rac*-lactide) revealed that the alkyl-aryloxide **3** exerts a moderate level of heteroselectivity (P_s= 0.68). More interestingly, this initiators **3** and **4** also allowed the well-controlled random copolymerization of ε-CL and L-LA as indicated by both the values of the reactivity ratios of the two comonomers (r_{CL} = 1.15 and 0.92, and r_{LA} = 1.37 and 1.05, for **3** and **4**, respectively), and the average lengths of the caproyl and lactidyl sequences (L_{CL} ~ 2.0; L_{LA} ~ 2.5, for both initiators). The copolymers also showed to possess monomer contents in close agreement with their composition in the initial monomer feed. Inspection by differential scanning calorimetry on the thermal properties such as T_g of various

copolymers produced by **3** revealed a strong dependence on monomer content, as these values vary linearly with the molar percentage of L-lactide unit in the copolymer over a temperature range of -30 to 42 ºC.

INTRODUCTION

The synthesis of aliphatic polyesters, such as polycaprolactone (PCL), poly(lactic acid)s (PLA), and their copolymers, is a topic of wide interest because of their important applications in packaging,[1] microelectronics,[2] and medical[3] fields. On this latter particular, among the most widely uses of these polymeric materials highlight biomedical and pharmaceutical applications such as heart tissue engineering,[4]biodegradable surgical sutures,[5]resorbableinternal fixation devices[5] and controlled drug release,[6]due to their physical properties and their nontoxic metabolic assimilation in humans.[7]The well-controlled ring-opening polymerization (ROP) of cyclic esters, such as *ε*-caprolactone (CL) and L- or D,L-lactide (L-/*rac*-LA), mediated by well-defined organo-metal catalysts can offer developed materials with high molecular weight, low polydispersity and controlled microstructure.[8]

The physical properties of PCL and PLA are quite different and in some way, complementary. Particularly, whereas PCL shows remarkable drug permeability, good elasticity, thermal properties and very low in vivo degradation rate (~1 year), in contrast, PLA presents very low drug permeability, poor elasticity, good mechanical properties and high in vivo degradation rate (~ few weeks).[9]On the bases of these antagonist features, the copolymerization of *ε*-CL and LA has recently attracted particular attention, given the possibility to fine tuning important polymer characteristic and prepared, as a result, advanced materials by controlling composition and distribution of these two comonomers through the polymer chain. A prove on the novelty on these

new materials is the very scarce number of specific reviews[10] and books[11] that have appeared until now.

For these reasons, there is clear demand for the synthesis of efficient catalysts for the successful copolymerization of ε-CL and LA. In this regards, different metal catalyst systems have been reported up to now, ranging from the traditional stannous octoate,[12]to rare earth[13]and main group catalysts (Al,[14a-d]Mg[14e]) as well as early transition metals (Ti[15]).However, very few have succeeded in the preparation of the strictly random copolymerization of these comonomer, *i.e.* with the average lengths of the caproyl and lactidyl sequences in adequate proportion (L_{CL}/ L_{LA}≈ 1). In addition, on this particular very few examples of effective initiators based on the biocompatible zinc metal have been successfully reported up to now. Indeed, the pioneering and elegant work of Darensbourg *et al.*[16]describes the employment of a bis(trimethylsylil)amide zinc-based complex containing a Schiff base derived from the natural amino acid phenylalanine for the production in the melt at 110ºC of a series of ε-CL/L-LA living-behaved random copolymers, with monomer content consistent with the initial mixture in the feed, medium-high molecular weights (M_n= 20 000-119 000 Da) and reasonable values of monomodal molecular weight distributions (PDI = 1.26 - 2.12). Secondly, Milione and Mazzeo*et al.*[17] recently reported a very interesting bis(trimethylsylil)amide zinc complex supported by a phosphido pincer ligand and its ability to promote ε-CL/L-LA random copolymerization, again in the melt at 110ºC, to achieve materials whose microstructure well reproduces the composition of the monomer feed, and show medium molecular weights (M_n = 32 000 Da) and expected polydispersity values (PDI = 2.3).

On the other hand, over the last few years our research group has made significant contributions in the preparation of efficient catalysts[18] for the well-controlled ROP of cyclic esters such as ε-CL and LAs. Given the biocompatible nature and the lack of toxicity to living tissue of these materials,

the employment of biocompatible metals such as magnesium[19] or zinc[20]for the synthesis of well-defined alkyl magnesium[21-24] and alkyl[22,25-28]-amide[29,30]and enantiopure mixed alkyl-/alkoxo/thioalkoxo[31]zinc complexes as highly effective single-component living initiators for the ROP of lactides, has stimulated our interest during this time.

As a result, some of these systems have been capable to produce both heterotactic[22-26,30]- and isotactic[27,28,31]-enriched PLA materials, with $P_s = 0.79$[23] and $P_i = 0.77$,[27,28] respectively, in a living fashion under mild conditions. In view of the growing interests on the search of more efficient catalysts based on the biocompatible zinc metal for the synthesis of ε-CL/LA copolymers having controlled composition and architecture, and considering our previous background in these homopolymerizations,[21-31] we addressed now the challenge of designing alternative zinc-based catalysts for the efficient homo- and random copolymerization of ε-CL and L-LA.

Herein, we report on the synthesis and structural characterization of a new family of chiral NNO alkyl and mixed ligand alkyl/alkoxo zinc complexes of the type [Zn(R)(κ^2-NNμ-O)Zn(R)$_2$] and [(ZnR)$_2$(κN:κN-μ-O)(μ-OAr)], respectively, and their application as single-component initiators in the living behaved ring-opening homo- and random copolymerization of ε-CL and L-LA.

RESULTS AND DISCUSSION

Reaction of chiral alcohol-scorpionate compound bpzteH[32] [bpzteH = 2,2-bis(3,5-dimethylpyrazol-1-yl)-1-*para*-tolylethanol] with [ZnR$_2$] (R = Me, CH_2SiMe_3) in a 1:2 molar ratio in toluene or diethyl ether afforded, after the appropriate work-up, the dinuclear chiral alkyl zinc complexes [Zn(R)(κ^2-NNμ-O)Zn(R)$_2$] (**1**–**2**) [κ^2-NNμ-O = bpzte, R = Me **1**, CH_2SiMe_3**2**], which were isolated as white solids in good yield (*ca*. 90%) (see Scheme 1).

We have explored some aspects concerning the reactivity of [Zn(R)(κ^2-NNμ-O)Zn(R)$_2$](**1**–**2**) with several aromatic alcohols and new complexes that contained aryloxide ligands were isolated. Thus, using these trialkyl complexes in an alcoholysis reaction with ArOH (1 equiv; Ar = 2,6-$C_6H_3Me_2$) yields the chiral dinuclear zinc complexes [(ZnR)$_2$(κN:κN-μ-O)(μ-OAr)] (**3**–**4**) [κN:κN-μ-O= bpzte, R = Me **3**, CH_2SiMe_3 **4**] as white solids in good yield (*ca*. 90%)(see Scheme 1). However, the reaction of **1**–**2** with aliphatic alcohols, such as methanol or isopropanol, in different molar ratios and under different conditions, proved unsuccessful.

Scheme 1. Synthesis of NNO-scorpionate alkyl zinc complexes (**1–4**).

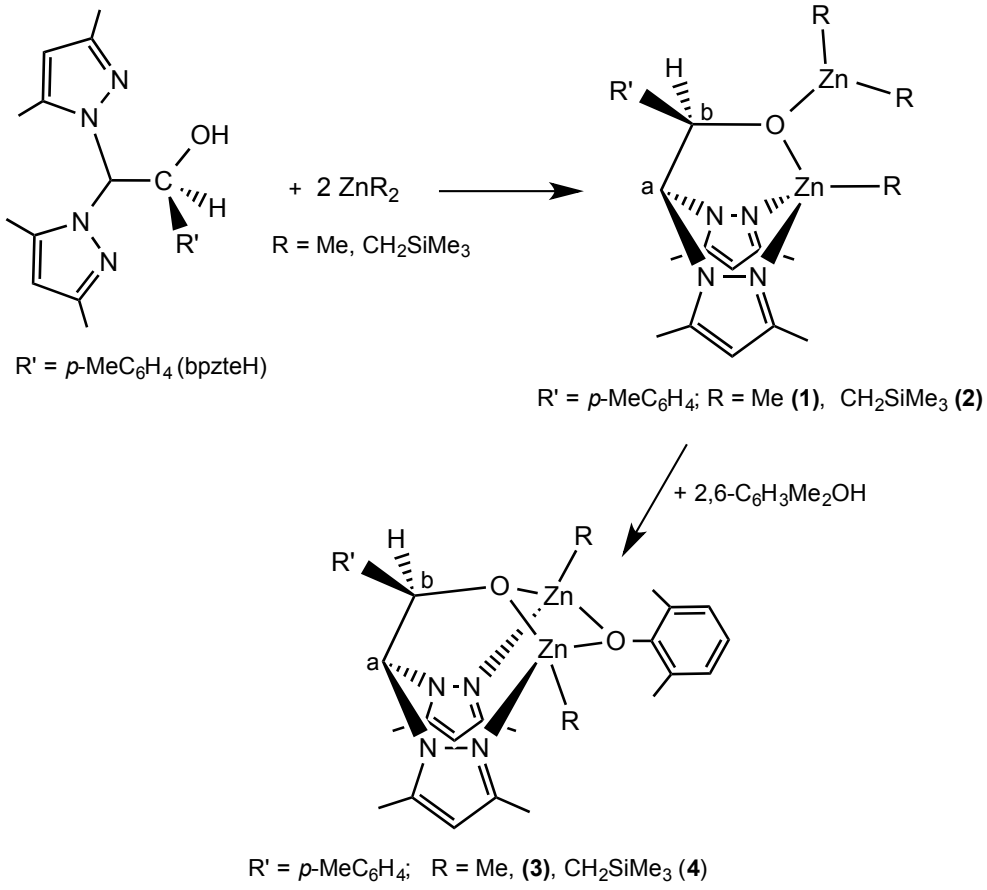

The different complexes were characterized spectroscopically. The ^{1}H and $^{13}C\{^{1}H\}$ NMR spectra of **1–4,** exhibit two distinct sets of pyrazole resonances, indicating the existence of two types of pyrazole ring. The ^{1}H NMR spectra of these complexes show two singlets for each of the H^{4}, Me^{3} and Me^{5}pyrazole protons, one broad singlet for each of the methine groups (the CH^{a} bridge of the two pyrazole rings and the chiral CH^{b}) and the signals corresponding to the R´ moieties of the scorpionate ligands and the alkyl oraryloxide ligands. These results are consistent with a geometric environment for the zinc atoms in which the two pyrazole rings are located in *cis* and *trans* positions with respect to the *p*-tolyl group (see Schemes 1).The ^{1}H NOESY-1D experiments enabled the unequivocal assignment of all ^{1}H resonances, and the assignment of the $^{13}C\{H\}$ NMR signals was carried out on the basis of ^{1}H-^{13}C heteronuclear correlation (g-HSQC) experiments. In addition, the presence in solution of racemic mixtures was confirmed by the addition of a chiral shift reagent, namely (*R*)-(–)-(9-anthryl)-2,2,2-trifluoroethanol, gave rise to the appearance in the ^{1}H NMR spectra of two signals for each proton, resulting from the two diastereoisomers of the corresponding two enantiomers.

Complexes **1** and**3** were also characterized by single-crystal X-ray diffraction and the molecular structures are shown in Figures 1 and 2, respectively. These studies confirmed that the presence in solution of the corresponding two enantiomers for **1** (*R* + *S*) is maintained in the solid-state. However, in complex**3** only one enantiomer was present in the unit cell although their ^{1}H NMR spectra (with the addition of a chiral shift reagent) correspond to both diastereoisomers from both enantiomers. The most representative bond lengths and angles are presented in Table1. (Crystallographic details are included in Table S1 in the SI).The complex **1** has a dinuclear structure in the solid state with a μ-bridging alkoxide in between the two four- and three-coordinate Zn(II) centers. The first zinc center Zn(1) has a distorted tetrahedral geometry with a

heteroscorpionate ligand that acts in a tridentate fashion. The pyrazolic nitrogens N(1) and N(3) occupy two positions and the alkoxide oxygen-bridge μ-O(1) and the alkyl group the other two positions. The second zinc center has a distorted trigonal geometry, in which μ-O(1) occupies one position and the alkyl groups the other two positions. The major distorsion in the tetrahedral Zn(1) was located in O(1)–Zn(1)–C(20) angle, which have values of 134.9(1)º. In addition, at the three-coordinated Zn center in the same complex, the values of the angleC(21)–Zn(2)–C(22) is145.2(1)º and this represent the major distortion. The X-ray structure analyses of complex **3** revealed that this molecule have a rhomboidal $(ZnO)_2$ core with clearly different Zn(1)–O(1) or O(2) and Zn(2)–O(1) or O(2) Å bond lengths, ranging from 1.97(1) to 2.05(1) Å, respectively, with the Zn···Zn diagonal (nearly 3 Å) much longer than the O···O diagonal (nearly 2.7 Å). The coordination environment of each Zn atom can be described as a distorted tetrahedron with a heteroscorpionate ligand that acts in a tridentate fashion (two coordinated pyrazole rings bridge the two zinc atoms and the oxygen atom from the alkoxide fragment, which also bridges the two zinc atoms), and the other two coordination positions of the two zinc atoms are completed with an oxygen atom from the aryloxide ligand bridging the two zinc atoms, and finally an alkyl ligand on each zinc atom. The dimeric aggregate is based on Zn_2O_2 four-membered rings, which have previously been observed in other zinc compounds that contain, for example, thiolate-oxo,[33] alkoxide-imino,[34] aryloxide[35] or aminoalcoholate[36] ligands and, more recently, in our research group with dinuclear complexes of the type $[Zn(R)(\kappa\text{-}NN\mu\text{-}O)]_2$.[26] Additionally, the Zn–O bond distance from the scorpionate ligand in this complex is similar to those in complex**1**, where the oxygen atoms also bridge the two zinc atoms. However, the Zn–N bond distances from the two pyrazole rings in this complex, where these rings bridge the two zinc atoms, are generally longer [nearly 2.13 Å] than

in complex**1**,where both pyrazole rings are coordinated in a chelating fashion to one zinc atom [nearly 2.10 Å].

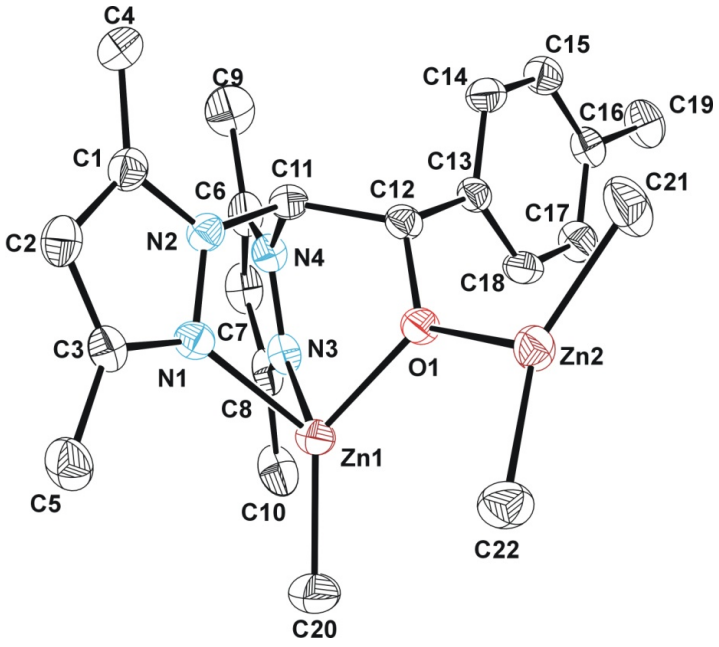

Figure 1. ORTEP view of the *S* enantiomer of [Zn(Me)(bpzte)Zn(Me)$_2$] (**1**). Hydrogen atoms have been omitted for clarity. Thermal ellipsoids are drawn at the 30% probability level.

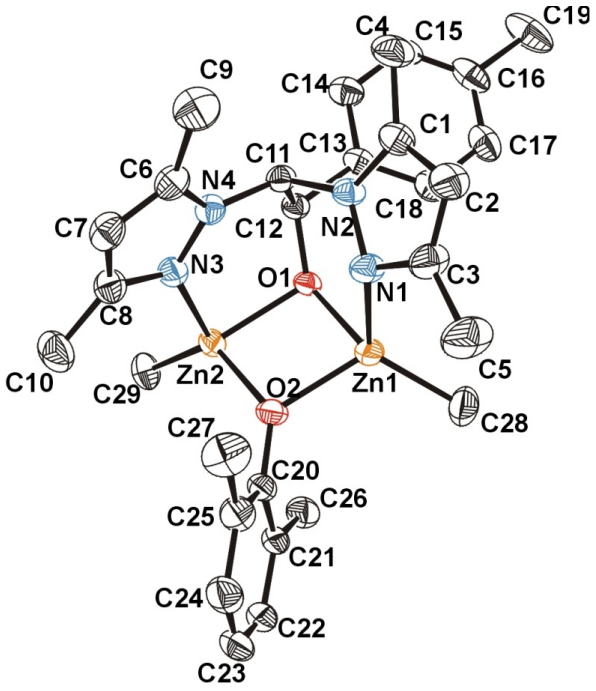

Figure 2. ORTEP view of the *R* enantiomer of [$(ZnMe)_2$(bpzte)(μ-OAr)] (**3**). Hydrogen atoms have been omitted for clarity. Thermal ellipsoids are drawn at the 30% probability level.

Table 1. Selected bond lengths (Å) and angles (°) for **1** and **3**.

	1		**3**
Bond lengths			
Zn(1)–O(1)	1.987(2)	Zn(1)–Zn(2)	2.9990(6)
Zn(1)–N(1)	2.111(2)	Zn(1)–O(1)	2.013(2)
Zn(1)–N(3)	2.106(2)	Zn(1)–O(2)	1.998(2)
Zn(1)–C(20)	1.957(3)	Zn(1)–N(1)	2.134(3)
Zn(2)–O(1)	2.052(2)	Zn(1)–C(28)	1.962(4)
Zn(2)–C(21)	1.979(3)	Zn(2)–O(1)	2.013(2)
Zn(2)–C(22)	1.970(3)	Zn(2)–O(2)	2.016(2)
O(1)–C(12)	1.392(3)	Zn(2)–N(3)	2.096(3)
		O(1)-C(12)	1.401(4)
		O(2)-C(20)	1.337(4)
		Zn(2)–C(29)	1.963(4)
Angles			
O(1)–Zn(1)–N(1)	85.67(7)	O(2)-Zn(1)–O(1)	83.74(9)
O(1)–Zn(1)–N(3)	91.51(7)	O(1)–Zn(1)–Zn(2)	41.86(6)
C(20)–Zn(1)–O(1)	134.9(1)	O(2)–Zn(1)–Zn(2)	41.88(7)
C(20)–Zn(1)–N(1)	124.9(1)	O(1)–Zn(2)–O(2)	83.29(9)
C(20)–Zn(1)–N(3)	119.8(1)	O(1)–Zn(2)–Zn(1)	41.86(7)
C(21)–Zn(2)–O(1)	107.8(1)	O(2)–Zn(2)–Zn(1)	41.43(6)
C(22)–Zn(2)–O(1)	107.0(1)	Zn(1)–O(1)–Zn(2)	96.3(1)
C(21)–Zn(2)–C(22)	145.2(1)	Zn(1)–O(2)–Zn(2)	96.7(1)
Zn(1)–O(1)–Zn(2)	122.09(8)		
C(12)–O(1)–Zn(1)	118.0(1)		
C(12)–O(1)–Zn(2)	116.7(1)		

Symmetry transformations used to generate equivalent atoms: [a] -x+1,-y,-z+2

Homopolymerization studies of *ε*-Caprolactone and Lactides.

Complexes **1**–**4** were assessed in the ring-opening polymerization of polar monomers such as *ε*-caprolactone (CL) and L-/*rac*-lactide (LA) under a nitrogen atmosphere and without the need for an activator, employing tetrahydrofuran as solvent. It was found that they acted as single-component living catalysts for the well-controlled polymerization of all monomers (see Table S2 in the SI). Inspection of the experimental M_n values of the polyesters produced reveals, as a common trend, that the molecular weights of the resulting polymer samples closely approximate the expected theoretical calculated values for one polymer chain per catalyst molecule on each monomer essay. Size exclusion chromatography (SEC) data for the resulting materials show monomodal weight distributions (see Figure S1), with very low polydispersity indexes.

Initiators **1** and **2** were assessed in the polymerization of CL, and it was found that the nature of the alkyl group affects the catalytic activity (CH_2SiMe_3 > Me),[37] where electronic effects predominate over the sterics (see Table S2 in the SI).

Furthermore, initiators **2–4** were systematically examined in tetrahydrofuran for the production of poly(lactides) (PLAs). In this case, the zinc alkyl derivative **2** polymerized L-LA under mild conditions (50 ºC) much faster than it did for the CL monomer. Interestingly, the NNO-donor alkyl-aryloxide catalysts **3** and **4** gave markedly increased productivity values since high conversions of monomer were achieved at 20 ºC. These reactions afforded highly crystalline, isotactic polymers (T_m = 169–177 ºC)[38] with low-medium molecular weight. The high level of control afforded by these initiators was further exemplified by initiator **3**, which gave rise to low polydispersity values in conjunction with linear correlations between M_n and percentage conversion (R^2 = 0.989) (see Figure S2 in the SI). A double-feed experiment reconfirmed the living behavior of catalyst **3** (see Table S2 in the SI, entries 10 and 11), which resulted in a polymer chain extension with very similar polymer features. Additionally, low molecular

weight materials produced by initiators **3** and **4** were studied by MALDI-ToF MS (see Figure S3 and the discussion in the SI). This finding provides evidence that the ring-opening of L-LA occurs by the initial addition of the aryloxide fragment, rather than the alkyl ligand, to the monomer in the materials produced.

Finally, initiators **2**–**4** were also tested in the polymerization of *rac*-lactide at 20 ºC and 50 ºC. While, the alkyl catalyst **2** proved to be active at 50 ºC, reaching high conversions after 4 hours and producing low molecular weight PLA materials with narrow polydispersity values, in contrast, the mixed ligand alkyl-aryloxide derivatives **3** and **4** proved to be active at room temperature and gave materials with similar polymer features. Poly(*rac*-lactide) microstructure analysis revealed that the alkyl-aryloxide **3** imparts a moderate level of heteroselectivity in the growing polymer chains (P_s up to 0.68, see Figure S4 in the SI), possibly by a chain end control mechanism.[39]

Copolymerization studies of *ε*-caprolactone and L-lactide.

Copolymerizations of *ε*-caprolactone and L-lactide were performed by employing compounds $[(ZnMe)_2(bpzte)(\mu\text{-}OAr)]$ (**3**) and $[(ZnCH_2SiMe_3)_2(bpzte)(\mu\text{-}OAr)]$ (**4**) under similar experimental conditions used for the homopolymerizations, but in toluene solution at 90°C, and varying the *ε*-CL/L-LA molar ratio. The obtained polymer samples were characterized by ^1H and ^{13}C NMR spectroscopy, GPC, and DSC analyses. The main results are summarized in Table 2.

Copolymerization runs initiated by **3** and **4** showed (Table 2), as expected, lower activity and needed longer reaction times and more energy conditions than that previously observed in the homopolymerization reactions of L-LA (see Table S2 in the SI). Not surprisingly, in all cases the materials produced show low molecular weights and polydispersities indexes slightly higher than that observed in the homocopolymerizations, possibly due to the higher reaction time and

temperature. However, these copolymerization reaction conditions are softer than that previously reported for the scarce number of zinc-based catalysts[16,17] examples employed for ε-CL/L-LA copolymerization (reactions performed in the melt at 110ºC during 30 min[16] or 1 h[17]).

The relative contents of each monomer in the copolymers were determined by ^{1}H NMR spectroscopy in $CDCl_3$, through the ratio of the integrated values of the methylene unit signals of the ε-CL proton in α and ε position around 2.35 ppm and 4.10 ppm, respectively (see Figure S5 in the SI). As a general trend, the copolymers composition parallels the initial ε-CL/L-LA molar ratio in the feed in all cases (Table 2). This feature is obviously expected when the full conversion is approaching, however it was also noticed at lower conversion runs. For instance, in the case of **3** the copolymerization of ε-CL/L-LA in a equimolar feed ratio (50/50) at 19% conversion of ε-CL and 20% conversion of L-LA produced a copolymer having 52% of "opened" L-LA units (entry 4, Table 2). A similar experiment carried out with extension of the reaction time up to 6 days and the same equimolecular feed ratio, also resulted in 54% of opened L-LA in the copolymer (entry 7, Table 2), and the obviously expected increase in the comonomers conversion (87% ε-CL; 89% L-LA). Analogous results were obtained employing compound **4** as catalyst, having bulkier alkyl substituents. However, lower polymerization rates were performed in this case, since after 48 h an equimolar feed ratio (50/50) produced similar monomer conversions than in 24 h by **3** (entries 12 and 4, respectively, Table 2) , resulting in analogous percentage of LA units in the copolymer. These findings suggest that the two monomers were homogeneously incorporated during the copolymerization process by employing both catalysts.

Table 2. Copolymerization of ε-Caprolactone and L-Lactide Catalyzed by 3 and 4.[a]

entry	Initiator	$[I]_0$:$[CL]_0$:$[LA]_0$ in the feed	Time (h)	Conv CL (%)[b]	Conv LA (%)[b]	LA in the copolymer (mol %)	$Ł_{CL}$[c]	$Ł_{LA}$[c]	$M_{n(theor)}$ (Da)[d]	$M_{n(exp.)}$ (Da)[e]	M_w/M_n[e]
1	**3**	1:20:80	48	32	30	85	1.0	11.1	4 200	4 600	1.23
2	**3**	1:40:60	48	27	25	65	1.0	5.9	3 400	3 500	1.24
3	**3**	1:50:50	18	14	22	53	1.9	2.8	2 400	2 500	1.24
4	**3**	1:50:50	24	19	20	52	2.0	2.3	2 500	2 850	1.24
5	**3**	1:50:50	32	25	26	51	1.9	2.5	3 300	3 700	1.26
6	**3**	1:50:50	48	27	29	52	1.8	2.7	3 600	3 500	1.28
7	**3**	1:50:50	144	87	89	54	2.2	2.5	13 000	13 400	1.31
8	**3**	1:60:40	48	10	6	39	2.5	1.5	1 000	3 300	1.27
9	**3**	1:80:20	48	7	2	21	3.0	1.1	n.d.	n.d.	n.d.
10	**4**	1:20:80	48	28	22	74	1.0	2.7	3 200	3 400	1.21
11	**4**	1:40:60	48	26	22	61	1.0	2.5	3 100	3 500	1.23
12	**4**	1:50:50	48	22	18	50	2.0	2.3	2 600	3 100	1.19
13	**4**	1:60:40	48	26	17	35	1.4	1.0	2 800	2 900	1.23
14	**4**	1:80:20	48	14	14	19	2.6	1.0	1 700	2 200	1.26

[a] Polymerization conditions: 90μmol of initiator, 22.5 mL of toluene as solvent at 90ºC; $([\varepsilon\text{-CL}]_0 + [\text{L-LA}]_0)/[I]_0 = 100$. [b] Percentage conversion of the monomer determined by ^{1}H NMR spectroscopy in $CDCl_3$. [c] Average sequences length of the caproyl unit and of the lactidyl unit as determined by ^{13}C NMR analysis.[13] [d] Theoretical $M_n = [\{([\varepsilon\text{-CL}]_0/[I]_0) \times (\%\text{ conversion of } \varepsilon\text{-CL}) \times (M_w \text{ of } \varepsilon\text{-CL})\} + \{([\text{L-LA}]_0/[I]_0) \times (\%\text{ conversion of L-LA}) \times (M_w \text{ of L-LA})\}]/100$. [e] Determined by size exclusion chromatography relative to polystyrene standards in tetrahydrofuran. Experimental M_n was calculated considering Mark–Houwink's corrections[40] for M_n [M_n(obsd) = 0.56 × M_n(GPC)].

A full detailed characterization of the copolymers chain microstructures was performed by ^{1}H NMR and ^{13}C-{^{1}H}-NMR analysis at diads and triads level. The percentage of CL−LA heterodiads were calculated by comparing, in the ^{1}H NMR spectrum, the intensity of the signals of the methylene protons close to the carbonyl of the CL−LA heterosequences with the same methylene protons for the CL−CL homosequences (protons in α position) (see Figure S5 in the SI). As expected, the increase of the amount of lactide in the initial monomer feed produces an increase in the amount of CL − LA heterodiads, suggesting a random copolymerization performance, while conversely, the CL-CL homodiads are those that increase. In addition, the analysis of the chain microstructures was also performed by inspection at triads level of the carbonyl region range (from 169 to 174 ppm) of the ^{13}C-{^{1}H}-NMR spectra of the obtained copolymers (Figure 3). Eight triads were observed accordingly to a binary copolymerization; four peaks between 173.55 and 172.80 ppm derived from the caproyl unit, and four additional peaks between 170.35 and 169.50 ppm attributed to the lactidyl unit, on the bases of the literature data.[13] It should be notice that the signal at 171 ppm, corresponding to the triad having one single “lactic” ester unit between two CL units, was never detected. That triad is indicative of transesterification reactions, since it cannot result from the insertion of the lactide monomer into the chain.[41] The absence of transesterification reactions was further exemplified by the narrow monomodal molecular weight distributions (M_w/M_n = 1.23-1.31), indicating that the copolymerization process mediated by both initiators occurs in a controlled manner.

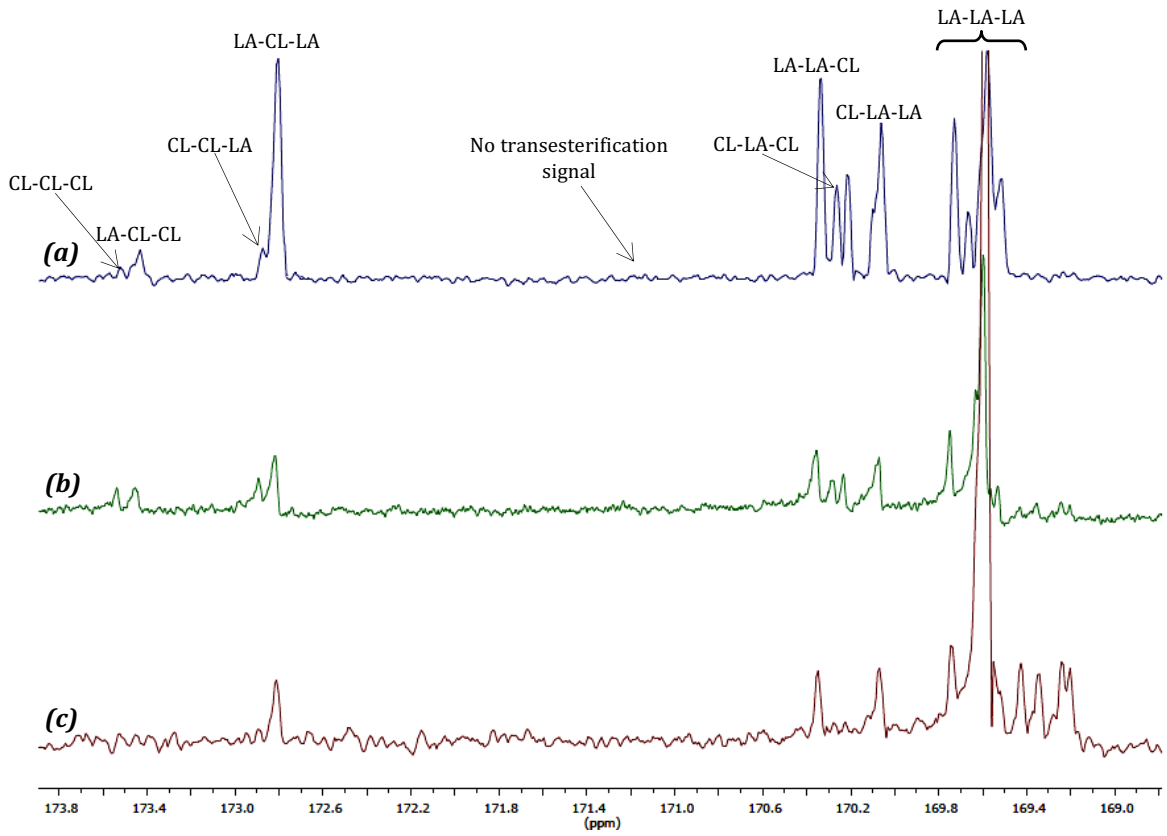

Figure 3: Carbonyl range of ^{13}C-$\{^1H\}$-*RMN* (400 MHz, 298 K, $CDCl_3$) of copolymers obtained for **3**: *(a)* entry 4 (50:50), *(b)* entry 2 (40:60), *(c)* entry 1 (20:80) (Table 2).

The average length of the caproyl (L_{CL}) and lactidyl (L_{LA}) sequences were also calculated from the integrals of the triads sequences signals according to the previously reported methods in the literature.[13]As a matter of fact, both the L_{CL} and L_{LA} parameters increased as the relative monomer amount in the feed increased for both catalysts. Moreover, for a 1:1 ratio of the comonomers in the feed, the L_{CL} and L_{LA} values were ~2, not only at low conversions (19% and 22% for ε-CL, and 20% and 18% for L-LA, entries 4 and 12, respectively, Table 2), but also approaching full conversion (87% and 89%, respectively, entry 7, Table 2). On the bases of these experimental features, a random copolymerization behavior can be newly suggested for both catalysts. In addition, the reactivity ratios r_{LA} and r_{CL} were also determined for both catalysts employing the Finneman-Ross method[14c] by carrying out copolymerizations of the monomer with different compositions (CL:LA ≈20:80, 40:60, 50:50,60:40 and 80:20) at low

conversions (<10%) (see Table S3 and Figure S6 in the SI). The values r_{CL} = 1.15 and 0.92, and r_{LA} = 1.37 and 1.05, for **3** and **4**, respectively, are indicative of a well-behaved random copolymerizations.

Finally, the thermal analysis of the properties of the copolymers prepared employing **3** were measured by differential scanning calorimetry (DSC) in the range from −50 to 200°C. The DSC thermograms of varying composition are provided in Figure S7 in the SI and the glass transition temperature parameters for polylactide, polycaprolactone, and their copolymers are listed in Table S4 in the SI. The obtained copolymers were amorphous. In all cases, the copolymer samples displayed unique glass transition temperature (T_g), with values intermediate between −60°C of pure poly(caprolactone) and 57°C of pure poly(L-LA) since, as anticipated, the thermal properties for the copolymers are very dependent on the composition of the monomers incorporated in the polymer chains. Expectedly, the T_g of the copolymers increased as the percent of lactide units in the copolymer increased. In addition, the experimental values of T_g fit reasonably well with the theoretical values calculated by the Fox law[42] (Figure 4). These data are a further support to the random structure of the copolymers.

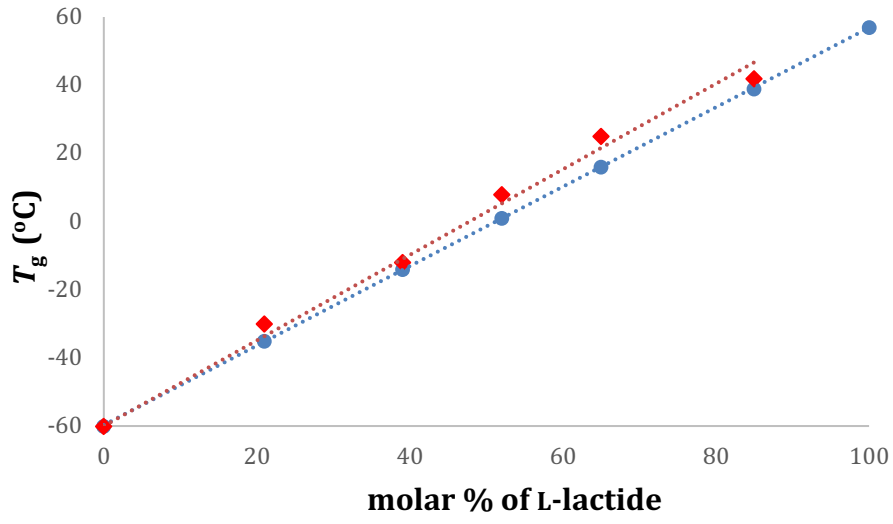

Figure 4. Plot of the experimental (red) (R^2 = 0.992) and theoretical (blue) T_g values of the ε-CL/L-LA copolymers as a function of the molar percentage of L-LA unit.

CONCLUSIONS

The reaction of a chiral bis(pyrazol-1-yl)methane-based NNO-donor scorpionate alcohol with [ZnR_2] has led to the preparation of new dinuclear zinc trisalkyls [$Zn(R)(\kappa^3\text{-NNO})Zn(R)_2$]. Using these complexes in an alcoholysis reaction with a phenol yielded mixed ligand alkyl/aryloxide complexes [$(ZnR)_2(\kappa N{:}\kappa N\text{-}\mu\text{-}O)(\mu\text{-}OAr)$]. The structures of these complexes were determined by ^{1}H and $^{13}C\{^{1}H\}$ NMR spectroscopy and, in addition, the single-crystal X-ray diffraction analysis of **1** and **3** also unambiguously confirmed the different dinuclear arrangements initially proposed for the two type of compounds.

Trisalkyl or alkyl-aryloxide zinc complexes behaved as single-site living initiators for the well-controlled homopolymerization of ε-CL and L-/*rac*-LA under mild conditions in few hours, producing materials with low molecular weights and narrow monomodal molecular weight distributions under mild conditions in only a few hours. In addition, microstructural analysis of poly(*rac*-lactide) indicates that **3** exerts a moderate degree of heteroactivity in the polymerization of *rac*-LA, with a P_s value up to 0.68. More interestingly, initiators **3** and **4** also promoted the random copolymerization of ε-CL and L-LA, as indicated by the reactivity ratio values (r_{CL} = 1.15 and 0.92, and r_{LA} = 1.37 and 1.05, for **3** and **4**, respectively) and the average lengths of the caproyl and lactidyl sequences (L_{CL} ~ 2.0; L_{LA} ~ 2.5, for both initiators). The copolymers obtained possess monomer contents in good agreement with the initial molar ratio in the monomer feed and narrow molecular weight distributions, suggesting a controlled behavior and the absence of detrimental transterification reactions during propagations. The analysis of the thermal properties in various copolymers obtained by **3** disclosed amorphous materials whose T_g values were modifiable in a linear fashion between −30 and 42°C by controlling the relative proportions of ε-CL and L-LA content.

EXPERIMENTAL SECTION

General Procedures

All manipulations were carried out under a nitrogen atmosphere using standard Schlenk techniques or a glovebox. Solvents were predried over sodium wire and distilled under nitrogen from sodium (toluene and *n*-hexane) or sodium-benzophenone (THF and diethyl ether). Deuterated solvents were stored over activated 4 Å molecular sieves and degassed by several freeze-thaw cycles.

The starting materials bdmpzm,[43] bpzteH,[32a] were also prepared according to literature procedures. Reagents $ZnMe_2$ (Aldrich) was used as purchased. $Zn(CH_2SiMe_3)_2$ was prepared according to literature procedures.[25,44] 2,6-Dimethylphenol was sublimed twice under reduced pressure and stored in a glovebox. L-Lactide and *rac*-lactide were sublimed twice, recrystallized from THF and finally sublimed again prior to use.

Instruments and Measurements

NMR spectra were recorded on a Varian Inova FT-500 spectrometer and are referenced to the residual deuterated solvent. ^{1}H NMR homodecoupled and NOESY-1D spectra were recorded on the same instrument with the following acquisition parameters: irradiation time 2 s and 256 scans, using standard VARIAN-FT software. 2D NMR spectra were acquired using the same software and processed using an IPC-Sun computer.

Microanalyses were performed with a Perkin-Elmer 2400 CHN analyzer. The specific rotation $[\alpha]_D^{22}$ was measured at a concentration of 0.1% w/v in toluene or chloroform at 22 ºC on a JASCO P2000 Polarimeter equipped with a sodium lamp operating at 589 nm with a light path length of 10 cm.

The molecular weights (M_n) and the molecular mass distribution (M_w/M_n) of polymer samples were measured byGel Permeation Chromatography (GPC) measurements performed on a

Shimadzu LC-20AD GPC equipped with a TSK-GEL G3000Hxl column and an ELSD-LTII light-scattering detector. The GPC column was eluted with THF at 40 ºC at 1 mL/min and was calibrated using eight monodisperse polystyrene standards in the range 580–483 000 Da.

MALDI-ToF MS data were acquired with a Bruker Autoflex II ToF/ToF spectrometer, using a nitrogen laser source (337 nm, 3 ns) in linear mode with a positive acceleration voltage of 20 kV. Samples were prepared as follows: PLA (20 mg) was dissolved in HPLC quality THF with matrix and NaI in a 100:5:5 ratio. Before evaporation, 10 μL of the mixture solution was deposited on the sample plate. External calibration was performed by using Peptide Calibration Standard II (covered mass range: 700–3 200 Da) and Protein Calibration Standard I (covered mass range: 5 000–17 500 Da). Every value was the average of two independent measurements.

The microstructures of PLA samples were determined by examination of the methine region in the homodecoupled ^{1}H NMR spectrum of the polymers recorded at room temperature in $CDCl_3$ on a Varian Inova FT-500 spectrometer with concentrations in the range 1.0 to 2.0 mg/mL.

PLA melting temperatures for the poly(L-lactide)s were measured using a melting point Block (SMP 10). The sample was heated at rate of 5 ºC/min up to 185 ºC and then, the sample is left to cool up to room temperature. After that, the sample was heated at rate of 2 ºC/min up to 185. This second step was carried out twice.

Glass transition temperature (T_g) measurements of the polymers were measured by differential scanning calorimetry (DSC) using a DSC-Q100 (TA Instruments) in nitrogen flow with a heating and cooling rate of $10°C \cdot min^{-1}$ in the range −50 to 200°C. Glass transition temperatures and melting temperatures were reported for the second heating cycle.

Preparation of complexes 1–4.

Synthesis of [Zn(Me)(bpzbe)Zn(Me)$_2$] (1). In a 250 cm^{3}Schlenk tube, bpzteH (1.0 g, 3.08 mmol) was dissolved in dry toluene (60 mL) and the solution was cooled to –70 ºC. A solution of $ZnMe_2$ (2.0 M in toluene, 3.10 mL, 6.16mmol) was added and the mixture was allowed to warm up to room temperature and stirred during 2 h. The solvent was evaporated to dryness under reduced pressure to yield a sticky white product. The product was washed with *n*-hexane (1 × 20 mL) to give compound **1** as colorless crystals from toluene at –26 ºC. Yield: 1.10 g (88%). ^{1}H NMR (C_6D_6, 297 K), δ 7.39 (d, 2H, $^3J_{H\text{-}H}$ = 7.7 Hz, *o*-H-Ph), 6.98 (d, 2H, $^3J_{H\text{-}H}$ = 7.7 Hz, *m*-H-Ph), 5.87 (bs, 2H, CH^b, CH^a), 5.40 (s, 1H, H$^{4'}$), 5.19 (s, 1H, H^4), 2.11 (s, 3H, Me$^{3'}$), 2.10 (s, 3H, Me^3), 2.09 (s, 3H, $\underline{CH_3}$-Ph), 1.61 (s, 3H, Me$^{5'}$), 1.14 (s, 3H, Me^5), 0.21 (s, 6H, Zn-($\underline{CH_3}$)$_2$), –0.20 (s, 3H, Zn-$\underline{CH_3}$). ^{13}C {^{1}H} NMR (C_6D_6, 297 K), δ 148.9–137.2 (C$^{3,3'}$, C$^{5,5'}$), 144.7 (*p*-C-Ph), 136.6 (*ipso*-C-Ph), 128.6 (*m*-C-Ph), 126.5 (*o*-C-Ph), 105.3 (C$^{4'}$), 104.5 (C^4), 81.9 (C^a), 70.7 (C^b), 20.9 ($\underline{CH_3}$-Ph), 13.5 (Me$^{3'}$), 12.5 (Me^3), 10.1 (Me$^{5'}$), 9.9 (Me^5), –2.5 (Zn-$\underline{CH_3}$), –15.6 (Zn-($\underline{CH_3}$)$_2$). Elemental analysis (%) calcd for $C_{22}H_{32}N_4OZn_2$: C, 52.92; H, 6.46; N, 11.22. Found: C, 52.95; H, 6.47; N, 11.19.

Synthesis of [Zn(CH_2SiMe_3)(bpzte)Zn(CH_2SiMe_3)$_2$] (2). The synthesis of **2** was carried out in an identical manner to **1**, but **2** was obtained as a white solid. bpzteH (1.0 g, 3.08 mmol), [Zn(CH_2SiMe_3)$_2$](1.8 M in Et_2O, 3.42 mL, 6.16 mmol). Yield: 1.96 g (89%). ^{1}H NMR (C_6D_6, 297 K), δ 7.10 (d, 2H, $^3J_{H\text{-}H}$ = 7.7 Hz, *o*-H-Ph), 6.95 (d, 2H, $^3J_{H\text{-}H}$ = 7.7 Hz, *m*-H-Ph), 5.70 (bs, 1H, CH^b), 5.57 (bs, 1H, CH^a), 5.41 (s, 1H, H$^{4'}$), 5.12 (s, 1H, H^4), 2.20 (s, 3H, Me$^{3'}$), 2.11 (s, 3H, $\underline{CH_3}$-Ph), 2.04 (s, 3H, Me^3), 1.63 (s, 3H, Me$^{5'}$), 1.07 (s, 3H, Me^5), 0.51 (s, 9H, Zn-$CH_2Si\underline{Me_3}$), 0.24 (s, 18H, Zn-($CH_2Si\underline{Me_3}$)$_2$), –0.11 (m, 2H, Zn-$\underline{CH_2}SiMe_3$), –0.55 (s, 4H, Zn-($\underline{CH_2}SiMe_3$)$_2$). ^{13}C {^{1}H} NMR (C_6D_6, 297 K), δ 149.7–139.1 (C$^{3,3'}$, C$^{5,5'}$), 141.2 (*p*-C-Ph), 137.2 (*ipso*-C-Ph), 129.1 (*m*-C-Ph), 127.8 (*o*-C-Ph), 106.1 (C$^{4'}$), 105.1 (C^4), 79.9 (C^a), 69.5 (C^b), 20.9 ($\underline{CH_3}$-Ph), 13.2 (Me$^{3'}$), 13.1 (Me$^{5'}$), 10.0 (Me^5), 9.5 (Me^3), 4.2 (Zn-$CH_2\underline{SiMe_3}$), 3.5 (Zn-($CH_2\underline{SiMe_3}$)$_2$), 0.2

(Zn-$\underline{CH_2}SiMe_3$), –9.02 (Zn-($\underline{CH_2}SiMe_3$)$_2$). Elemental analysis (%) calcd for $C_{31}H_{56}N_4OSi_3Zn_2$: C, 52.01; H, 7.88; N, 7.83. Found: C, 52.06; H, 7.92; N, 7.79.

Synthesis of [(ZnMe)$_2$(bpzte)(OAr)] (3). In a 250 cm^{3}Schlenk tube, [Zn(Me)(bpzte)Zn(Me)$_2$] (**1**) (1.0 g, 2.0 mmol) was dissolved in dry toluene (60 mL) and the solution was cooled to –70 ºC. In another 100 mL Schlenk tube, 2,6-dimethylphenol (0.24 g, 2.0mmol) was dissolved in dry toluene (20 mL) and precooled to –20 ºC. The solution of 2,6-dimethylphenol was added dropwise to the [Zn(Me)(bpzbe)Zn(Me)$_2$]solution and the mixture was allowed to warm up to room temperature and stirred during 10 min. The solvent was evaporated to dryness under reduced pressure to yield a pale yellow product, which was recrystallized from a mixture of toluene/*n*-hexane (1:3) at –26 ºC to give colorless crystals. Yield: 1.12 g (92%). ^{1}H NMR (C_6D_6, 297 K), δ 7.21 (d, 2H, $^3J_{H\text{-}H}$ = 7.7 Hz, *o*-H-Ph), 7.16 (d, 2H, $^3J_{H\text{-}H}$ = 7.1 Hz, *m*-H-OAr), 7.00 (d, 2H, $^3J_{H\text{-}H}$ = 7.7 Hz, *m*-H-Ph), 6.85 (t, 1H, $^3J_{H\text{-}H}$ = 7.1 Hz, *p*-H-OAr), 5.98 (bs, 1H, CH^b), 5.50 (bs, 1H, CH^a), 5.40 (s, 1H, H$^{4'}$), 5.16 (s, 1H, H^4), 2.50 (bs, 6H, $\underline{CH_3}$-OAr), 2.11 (s, 3H, $\underline{CH_3}$-Ph), 2.05 (s, 3H, Me^3), 1.95 (s, 3H, Me$^{3'}$), 1.26 (s, 3H, Me$^{5'}$), 1.08 (s, 3H, Me^5), –0.05 (bs, 3H, Zn-$\underline{CH_3}$), –0.30 (bs, 3H, Zn-$\underline{CH_3}$).^{13}C {^{1}H} NMR (C_6D_6, 297 K), δ 160.3 (C_{ipso}-OAr), 154.2–140.0 (C$^{3,3'}$, C$^{5,5'}$), 143.2 (*p*-C-Ph), 137.9 (C_{ipso}-Ph), 128.6 (*o*-C-OAr), 128.3 (*m*-C-Ph), 126.5 (*p*-C-OAr), 125.6 (*o*-C-Ph), 118.3 (*m*-C-OAr), 107.6 (C$^{4'}$), 107.5 (C^4), 77.4 (C^a), 71.8 (C^b), 21.2 ($\underline{CH_3}$-Ph), 17.9 ($\underline{CH_3}$-OAr), 13.8 (Me$^{3'}$), 13.2 (Me^3), 10.7 (Me$^{5'}$), 10.5 (Me^5), –14.2 (Zn-$\underline{CH_3}$), –14.4 (Zn-$\underline{CH_3}$). Elemental analysis (%) calcd for $C_{29}H_{38}N_4O_2Zn_2$: C, 57.53; H, 6.33; N, 9.25. Found: C, 57.48; H, 6.35; N, 9.29.

Synthesis of [(ZnCH$_2$SiMe$_3$)$_2$(bpzte)(OAr)] (4). The synthesis of **4** was carried out in an identical manner to **3**, but **4** was obtained as a white solid. [Zn(CH$_2$SiMe$_3$)(bpzte)Zn(CH$_2$SiMe$_3$)$_2$] (**2**) (1.0 g, 1.40 mmol), 2,6-dimethylphenol (0.17 g, 1.40 mmol). Yield: 0.93 g (89%). ^{1}H NMR (C_6D_6, 297 K), δ 7.19 (d, 2H, $^3J_{H\text{-}H}$ = 7.7 Hz, *o*-H-

Ph), 7.14 (d, 2H, $^{3}J_{H\text{-}H}$ = 7.1 Hz, *m*-H-OAr), 6.99 (d, 2H, $^{3}J_{H\text{-}H}$ = 7.7 Hz, *m*-H-Ph), 6.82 (t, 1H, $^{3}J_{H\text{-}H}$ = 7.1 Hz, *p*-H-OAr), 6.16 (bs, 1H, CH^{b}), 5.51 (bs, 1H, CH^{a}), 5.42 (s, 1H, $H^{4'}$), 5.27 (s, 1H, H^{4}), 2.38 (bs, 6H, $\underline{CH_3}$-OAr), 2.11 (s, 3H, $\underline{CH_3}$-Ph), 2.06 (s, 3H, Me^{3}), 2.02 (s, 3H, $Me^{3'}$), 1.21 (s, 3H, $Me^{5'}$), 1.08 (s, 3H, Me^{5}), 0.34 (s, 9H, Zn-$CH_2\underline{SiMe_3}$), 0.25 (s, 9H, Zn-$CH_2\underline{SiMe_3}$), –0.28 (d, 1H, $^{2}J_{H\text{-}H}$ = 12.3 Hz, Zn-$\underline{CH_2}SiMe_3$), –0.47 (d, 1H, $^{2}J_{H\text{-}H}$ = 12.3 Hz, Zn-$\underline{CH_2}SiMe_3$), –0.62 (d, 1H, $^{2}J_{H\text{-}H}$ = 12.3 Hz, Zn-$\underline{CH_2}SiMe_3$), –0.73 (d, 1H, $^{2}J_{H\text{-}H}$ = 12.3 Hz, Zn-$\underline{CH_2}SiMe_3$). ^{13}C {^{1}H} NMR (C_6D_6, 297 K), δ 159.3 (C_{ipso}-OAr), 152.2–141.2 ($C^{3,3'}$, $C^{5,5'}$), 143.1 (*p*-C-Ph), 137.6 (C_{ipso}-Ph), 128.2 (*o*-C-OAr), 128.3 (*m*-C-Ph), 126.1 (*p*-C-OAr), 125.7 (*o*-C-Ph), 118.2 (*m*-C-OAr), 107.6 ($C^{4'}$), 107.3 (C^{4}), 76.3 (C^{a}), 70.6 (C^{b}), 20.8 ($\underline{CH_3}$-Ph), 16.9 ($\underline{CH_3}$-OAr), 13.5 ($Me^{3'}$), 13.3 (Me^{3}), 10.5 ($Me^{5'}$), 10.2 (Me^{5}), 2.3 (Zn-$CH_2\underline{SiMe_3}$), 1.6 (Zn-$CH_2\underline{SiMe_3}$), –7.0 (Zn-$\underline{CH_2}SiMe_3$), –7.9 (Zn-$\underline{CH_2}SiMe_3$). Elemental analysis (%) calcd for $C_{35}H_{54}N_4O_2Si_2Zn_2$: C, 56.06; H, 7.26; N, 7.47. Found: C, 56.00; H, 7.30; N, 7.45.

General Homopolymerization Procedures. Polymerizations of ε-CL, L-LA and *rac*-LA were performed on a Schlenk line in a Schlenk tube equipped with a magnetic stirrer. The Schlenk tubes were charged in the glovebox with the required amount of monomer and initiator, separately, and then attached to the vacuum line. The initiator and the monomer were dissolved in the appropriate amount of solvent, and temperature equilibration was ensured in both Schlenk tubes by stirring the solutions for 15 min in a bath. The appropriate amount of initiator was added by syringe, and polymerization times were measured from that point. Polymerizations were stopped by injecting a solution of hydrochloric acid in methanol(5%). Polymers were precipitated in methanol, filtered off, redissolved in tetrahydrofuran and reprecipitated in methanol and finally dried in vacuo to constant weight.

General Copolymerization Procedures. In a typical preparation, the polymerization experiments were performed on a Schlenk line in a Schlenk tube equipped with a magnetic

stirrer. The Schlenk tubes were charged in the glovebox with the desired ratio of ε-CL/L-LA and initiator, separately, and then attached to the vacuum line. The initiator and the comonomers were dissolved in the appropriate amount of toluene and heated up to the required temperatureby stirring the solutions for 15 min in a bath. The appropriate amount of initiator was added by syringe, and polymerization times were measured from that point. Polymerizations were stopped by injecting a solution of hydrochloric acid in methanol(5%). The copolymers were precipitated in methanol, filtered off, redissolved in tetrahydrofuran and precipitated in methanol and finally dried in vacuo to constant weight.

X-ray Crystal Structure Determination: Single crystals of **1** and **3** were mounted on a glass fiber and transferred to a Bruker X8 APEX II diffractometer with graphite-monochromated Mo-Kα radiation (λ = 0.71073 Å) and equipped with an Oxford CryosystemsCryostream Cooler Device. Data were integrated using the SAINT[45] program and were corrected for absorption effects with the semi-empirical from equivalents method using SADABS.[46] Details of crystal data, data collection, and refinement can be found in Table S1 in ESI†. The structures were solved by direct methods and refined on F^2 by full-matrix least squares using the software package SHELXTL version 6.10.[47] All non-hydrogen atoms were refined with anisotropic displacement coefficients. All hydrogen atoms were added to their geometrically ideal positions. During the structural refinement of **1**, the disordered solvent (C_5H_{12}) was squeezed.[48] The crystal data reported earlier in this paper are given without the contribution of the disordered solvent.

Acknowledgments

We gratefully acknowledge financial support from the Ministerio de Economia y Competitividad (MINECO), Spain (Grants No. CTQ2011-22578/BQU and CTQ2014-51912-REDC) and from URJC-Banco Santander, Spain (Grant No. GI_EXCELENCIA, QUINANOAP).

Supporting Information: Details of crystal data and structure refinement for **1** and **3** and details of the ring opening homo- and copolymerization of ε-CL and L-LA studies. This material is available free of charge via the Internet at http://pubs.acs.org.

References

(1) (a) Vacanti, J. P.; Langer, R.; Upton, J.; Marler, J. J. *Adv Drug Deliv Rev.* **1998**, *33*, 165-182. (b) Frazza, E. J.; Schmitt, E. E. *Journal of Biomedical Materials Research* **1971**, *5*, 43-58. (c) Dexon and Vicryl are products of Davis & Geek Corp., Wayne, NJ, and Ethicon, Inc., Somerville, NJ, respectively.

(2) (a) Penco, M.; Donetti, R.; Mendichi, R.; Ferruti, P. *Macromol. Chem. Phys.* **1998**, *199*, 1737-1745. (b) Kim, H.; Sung, Y. K.; Jung, J.; Baik, H.; Min, T. J.; Kim, Y. S. *J. Korean Chem. Soc.* **1990**, *34*, 203-210.

(3) Darensbourg, D. J.; Choi, W.; Richers, C. P. *Macromolecules* **2007**, *40*, 3521-3523.

(4) (a) Pêgo, A. P.; Siebum, B.; VanLuyn, M. J. A.; Gallego, X. J.; Van Seijen, Y.; Poot, A. A.; Grijpma, D. W.; Feijen, J. *Tissue Eng.* **2003**, *9*, 981–994.

(5) Beiser, I. H.; Konat, I. O. *J. Am. Podiatric Med. Assoc.* **1990**, *80*, 272–275.

(6) (a) Leupron Depot is a product of Takeda Chemical Industries, Ltd., Japan, for drug delivery purposes. (b) Smith, A.; Hunneyball, I. M. *Int. J. Pharm.* **1986**, *30*, 215–220.

(7) (a) Ragauskas, A. J.; Williams, C. K.; Davison, B. H.; Britovsek, G.; Cairney, J.; Eckert, C. A.; Frederick, W. J., Jr.; Hallett, J. P.; Leak, D. J.; Liotta, C. L.; Mielenz, J. R.; Murphy, R.; Templer, R.; Tschaplinski, T. *Science* **2006**, *311*, 484-9. (b) Ghosh, S. *J. Chem. Res.* **2004**, 241–246.

(8) Selected reviews: (a) Sarazin, Y.; Carpentier, J.-F.*Chem. Rev.*, **2015**, *15*, 3564–3614. (b) Dove, A. P.*ACS Macro Lett.*, **2012**, *1*, 1409–1412. (c) Dijkstra, P. J.; Du, H.; Feijen, *J. Polym. Chem.***2011**, *2*, 520−527. (d) Thomas, C. M. *Chem. Soc. Rev.* **2010**, *39*, 165−173. (e) Arbaoui, A.; Redshaw, C. *Polym. Chem.* **2010**, *1*, 801−826. (f) Platel, R. H.; Hodgson, L. M.; Williams, C. K. *Polym. Rev.* **2008**, *48*, 11−63. (g) Dechy-Cabaret, O.; Martin-Vaca, B.; Bourissou, D. *Chem. Rev.* **2004**, *104*, 6147−6176. (h) O'Keefe, B. J.; Hillmyer, M. A.; Tolman, W. B. *J. Chem. Soc., Dalton Trans.* **2001**, 2215−2224.

(9) (a) Albertsson, A. C.; Varma, I. K. *Biomacromolecules* **2003**, *4*, 1466−1486. (b) Chiellini, E.; Solaro, R. *Adv. Mater.***1996**, *8*, 1375−1381. (c) Schindler, A.; Jeffcoat, R.; Kimmel, G. L.; Pitt, C. G.; Wall, M. E.; Zweidinger, R. In Contemporary Topics in Polymer Science; Pearce, E. M., Schaefgen, J. R., Eds.; Plenum: New York, 1977; Vol. 2, p 251.

(10) Cameron, D. J. A.; Shaver, M. P. *Chem. Soc. Rev.* **2011**, *40*, 1761–1776.

(11) For books in this area see: (a) Auras, R.; Lim, L.-T. *Poly(lactic acid): synthesis, structures, properties, processing, and applications.* Wiley: Hoboken, NJ, 2010, Chapter 4, pp 43–58. (b) Abraham J. Domb, Joseph Kost, David M. Wiseman, *Handbook of Biodegradable Polymers.* (c) H. Abe, Y. Doi, In Biopolymers: Polyesters II—Properties and Chemical Synthesis; A. Steinb€uchel, Y. Doi, Eds.; Wiley-VCH: Weinheim, 2002; Vol. 3b, Chapter 5, pp 105–132.

(12) (a) Baimark, Y.; Molloy, R. *ScienceAsia* **2004**, *30*, 327−334. (b) Faÿ, F.; Renard, E.; Langlois, V.; Linossier, I.; Vallée-Rehel, K. *Eur. Polym. J.* **2007**, *43*, 4800−4813.

(13) Shen, Y.; Zhu, K. J.; Shen, Z.; Yao, K.-M. *J. Polym. Sci. Pol. Chem.* **1996**, *34*, 1799−1805.

(14) (a) Li, L.; Liu, B.; Liu, D.; Wu, C.; Li, S.; Liu, B.; Cui, D. *Organometallics*, **2014**, *33*, 6474–6480. (b) Castro-Osma, J. A.; Alonso-Moreno, C.; Márquez-Segovia, I.; Otero, A.; Lara-Sánchez, A.; Fernández-Baeza, J.; Rodríguez, A. M.; Sánchez-Barba, L. F.; García-Martínez, J. C. *Dalton Trans*., **2013**, *42*, 9325–9337. (c) Li, G.; Lamberti, M.; Pappalardo, D.; Pellecchia, C. *Macromolecules* **2012**, *45*, 8614−8620. (d) Nomura, N.; Akita, A.; Ishii, R.; Mizuno, M., *J. Am. Chem. Soc.*, **2010**, *132*, 1750–1751. (e) Wei, Z.; Liu, L.; Qu, C.; Qi, M. *Polymer*, **2009**, *50*, 1423–1429.

(15) Dakshinamoorthy, D.; Peruch, F.*J. Polym. Sci. Pol. Chem.* **2012**, *50*, 2161–2171.

(16) Darensbourg, D. J.; Karroonnirun., O. *Macromolecules* **2010**, *43*, 8880−8886.

(17) D'Auria, I.; Lamberti, M.; Mazzeo, M.; Milione, S.; Roviello, G.; Pellecchia, C.; *Chem. Eur. J.* **2012**, *18*, 2349 – 2360.

(18) Otero, A.; Fernández-Baeza, J.; Lara-Sánchez, A.; Sánchez-Barba, L. F. *Coord. Chem. Rev.* **2013**, *257*, 1806–1868.

(19) (a) Cowan, J. A. *The biological chemistry of magnesium*. VCH Publishers: 1995. (b) Campbell, N. A. Biology. Benjamin/Cummings Pub. Co.: Redwood City, Calif., 1993; p 718 and 811.

(20) (a) Parkin, G. *Chem*. *Commun*. **2000**, 1971–1985. (b) Mills, C. F., *Zinc in human biology*. Springer-Verlag: London, 1989.

(21) Sánchez-Barba, L. F.; Garcés, A.; Fajardo, M.; Alonso-Moreno, C.; Fernández-Baeza, J.; Otero, A.; Antiñolo, A.; Tejeda, J.; Lara-Sánchez, A.; López-Solera, M. I. *Organometallics* **2007**, *26*, 6403–6411.

(22) (a) Garcés, A.; Sánchez-Barba, L. F.; Alonso-Moreno, C.; Fajardo, M.; Fernández-Baeza, J.; Otero, A.; Lara-Sánchez, A.; López-Solera, I.; Rodríguez, A. M. *Inorg. Chem.* **2010**, *49*, 2859–2871. (b) Otero, A.; Fernández-Baeza, J.; Antiñolo, A.; Lara-Sánchez, A.; Martínez-Caballero, E.; Tejeda, J.; Sánchez-Barba, L. F.; Alonso-Moreno, C.; López-Solera, I. *Organometallics* **2008**, *27*, 976–983.

(23) Sánchez-Barba, L. F.; Garcés, A.; Fernández-Baeza, J.; Otero, A.; Alonso-Moreno, C.; Lara-Sánchez, A.; Rodríguez, A. M. *Organometallics* **2011**, *30*, 2775–2789.

(24) (a) Garcés, A.; Sánchez-Barba, L. F.; Fernández-Baeza, J.; Otero, A.; Honrado, M.; Lara-Sánchez, A.; Rodríguez, A. M. *Inorg. Chem*. **2013**, *52*, 12691−12701. (b) Sánchez-Barba, L. F.; Garcés, A.; Fernández-Baeza, J.; Otero, A.; Honrado, M.; Lara-Sánchez, A.; Rodríguez, A. M.; López-Solera I. *Eur. J. Inorg. Chem.* **2014**, 1922–1928.

(25) Alonso-Moreno, C.; Garcés, A.; Sánchez-Barba, L. F.; Fajardo, M.; Fernández-Baeza, J.; Otero, A.; Lara-Sánchez, A.; Antiñolo, A.; Broomfield, L.; López-Solera, M. I.; Rodríguez, A. M. *Organometallics* **2008**, *27*, 1310–1321.

(26) Otero, A.; Fernández-Baeza, J.; Sánchez-Barba, L. F.; Tejeda, J.; Honrado, M.; Garcés, A.; Lara-Sánchez, A.; Rodríguez, A. M. *Organometallics* **2012**, *31*, 4191–4202.

(27) Honrado, M.; Otero, A.; Fernández-Baeza, J.; Sánchez-Barba, L. F.; Lara-Sánchez, A.; Tejeda, J.; Carrión, M. P.; Martínez-Ferrer, J.; Garcés, A.; Rodríguez, A. M. *Organometallics* **2013**, *32*, 3437–3440.

(28) Honrado, M.; Otero, A.; Fernández-Baeza, J.; Sánchez-Barba, L. F.; Garcés, A.; Lara-Sánchez, A.; Martínez-Ferrer, J.; Sobrino, S.; Rodríguez, A. M. *Organometallics* **2015**, *34*, 3196−3208.

(29) Sánchez-Barba, L. F.; Alonso-Moreno, C.; Garcés, A.; Fajardo, M.; Fernández-Baeza, J.; Otero, A.; Lara-Sánchez, A.; Rodriguez, A. M.; López-Solera, I. *DaltonTrans*. **2009**, 8054–8062.

(30) Honrado, M.; Otero, A.; Fernández-Baeza, J.; Sánchez-Barba, L. F.; Garcés, A.; Lara-Sánchez, A.; Rodríguez, A. M. *Dalton Trans.* **2014**, *43*, 17090–17100.

(31) Honrado, M; Otero, A.; Fernández-Baeza, J.; Sánchez-Barba, L. F.; Garcés, A.; Lara-Sánchez, A.; Rodríguez,A. M. *Organometallics*, **2014**, *33*, 1859-1866.

(32) (a) Otero, A.; Fernández-Baeza, J.; Tejeda, J.; Lara-Sánchez, A.; Sánchez-Molina, M.; Franco, S.; López-Solera, I.; Rodríguez, A. M.; Sánchez-Barba, L. F.; Morante-Zarcero, S.; Garcés, A. *Inorg. Chem*. **2009**, *48*, 5540–5554. (b) Otero, A.; Fernández-Baeza, J.; Antiñolo, A.; Tejeda, J.; Lara-Sánchez, A.; Sánchez-Barba, L. F.; Sánchez-Molina, M.; Franco, S.; López-Solera, M. I.; Rodríguez, A. M. *Inorg. Chem*. **2007**, *46*, 8475–8477. (c) Otero, A.; Fernandez-Baeza, J.; Antiñolo, A.; Tejeda, J.; Lara-Sanchez, A.; Sanchez-Barba, L.; Expósito, M. T.; Rodriguez, A. M. *Dalton Trans*. **2003**, 1614–1619.

(33) Boyle, T. J.; Pratt, H. D.; Alam, T. M.; Headley, T.; Rodriguez, M. A.*Eur. J. Inorg. Chem.* **2009**, 855-865.

(34) Grunova, E.; Roisnel, T.; Carpentier, J.-F.*Dalton Trans.* **2009**, 9010-9019.

(35) Poirier, V.; Roisnel, T.; Carpentier, J.-F.; Sarazin, Y.*Dalton Trans.* **2009**, 9820-9827.

(36) Johnson, A. L.; Hollingsworth, N.; Kociok-Köhn, G.; Molloy, K. C.*Inorg. Chem.* **2008**, *47*, 12040-12048.

(37) Simoes, J. A. M.; Beauchamp, J. L.*Chem. Rev.* **1990**, *90*, 629-688.

(38) (a) Becker, J. M.; Pounder, R. J.; Dove, A. P.*Macromol. Rapid Commun.* **2010**, *31*, 1923-1937; (b) Zhong, Z.; Dijkstra, P. J.; Feijen, J. *J. Am. Chem. Soc.* **2003**, *125*, 11291-11298; (c) Radano, C. P.; Baker, G. L.; Smith, M. R. *J. Am. Chem. Soc.* **2000**, *122*, 1552-1553.

(39) Nomura, N.; Ishii, R.; Yamamoto, Y.; Kondo, T. *Chem.* –Eur. *J.* **2007**, *13*, 4433-4451.

(40) (a) Baran, J.; Duda, A.; Kowalski, A.; Szymanski, R.; Penczek, S. *Macromol. Rapid* Commun. **1997**, *18*, 325-333. (b) Barakat, I.; Dubois, P.; Jérôme, R.; Teyssié, P., *J. Polym. Sci. Pol. Chem.* **1993**, *31*, 505-514.

(41) Vanhoorne, P.; Dubois, P.; Jerome, R.; Teyssie, P. *Macromolecules***1992**, *25*, 37−44.

(42) (a) Barba, A. A.; Dalmoro, A.; De Santis, F.; Lamberti, G. *Polym. Bull*. **2009**, *62*, 679−688. (b) Fox, T. G.; Flory, P. J. *J. Appl. Phys*. **1950**, *21*, 581−591.

(43) (a) Diez-Barra, E.; de la Hoz, A.; Sanchez-Migallon, A.; Tejeda, J., *J. Chem. Soc., Perkin Trans. 1* **1993**, 1079-1083; b) Juliá, S.; Sala, P.; Del Mazo, J.; Sancho, M.; Ochoa, C.; Elguero, J.; Fayet, J.-P.; Vertut, M.-C., *J. Heterocycl. Chem.* **1982**, *19*, 1141-1145.

(44) Chisholm, M. H.; Huffman, J. C.; Phomphrai, K.*J. Chem. Soc., Dalton Trans.* **2001**, 222-224.

(45) SAINT+ v7.12a. Area-Detector Integration Program. Bruker-Nonius AXS. Madison, Wisconsin, USA, 2004.

(46) Sheldrick, G. M. SADABS version 2004/1. A Program for Empirical Absorption Correction. University of Göttingen, Göttingen, Germany, 2004.

(47) SHELXTL-NT version 6.12. Structure Determination Package. Bruker-Nonius AXS. Madison, Wisconsin, USA, 2001.

(48) Spek, A. *J. Appl. Crystallogr.* **2003**, *36*, 7-13.

GRAPHIC TABLE OF CONTENTS ENTRY

Copolymerization of Cyclic Esters Controlled by Chiral NNO-Scorpionate Zinc Initiators.

Antonio Otero,[*,†] *Juan Fernández-Baeza,*[*,†] *Luis F. Sánchez-Barba,*[*,‡] *Manuel Honrado,*[†] *Andrés Garcés,*[‡] *Agustín Lara-Sánchez*[†] *and Ana M. Rodríguez*[†]

A series of chiral dinuclear alkyl-aryloxide-containing zinc heteroscorpionates of the type [(ZnR)$_2$(κN:κN-μ-O)(μ-OAr)] act as single-component initiators for the ring-opening homopolymerization of ε-CL and L-LA, exerting a moderate level of heteroselectivity (P_s = 0.68). These initiators also promote the well controlled random copolymerization of both monomers, with monomer contents in the materials in agreement with the initial feed and T_g values with strong dependence on monomer content.